QUANTIFYING COOPERATIVE BINDING OF CHOLERA TOXIN B WITH GANGLIOSIDES

A Thesis

by

PRATIK KRISHNAN

Submitted to the Office of Graduate and Professional Studies of
Texas A&M University
in partial fulfillment of the requirements for the degree of

MASTER OF SCIENCE

Chair of Committee,	Hung-Jen Wu
Committee Members,	M.M Faruque Hasan
	Arul Jayaraman
Head of Department,	M. Nazmul Karim

August 2016

Major Subject: Chemical Engineering

ABSTRACT

Many biochemical processes involve binding between carbohydrates and biomolecules on the surface of cells. These may involve multivalent interactions that can considerably alter the binding specificity and avidity of biomolecules. A novel nanocube sensor has been developed to elucidate the cooperativity in binding of biomolecules to carbohydrates. A fluidic supported lipid bilayer coated on the nanocube sensor allows this system to mimic a cell membrane *in vitro.* Cholera toxin B (CTB) subunit has been taken as a model system and its binding with several gangliosides has been demonstrated using this sensor. The amount of CTB bound to the lipid bilayer is then quantified by observing the shifts in the quadrupolar localized surface plasmon resonance peak using a standard laboratory spectrometer.

The ultimate objective of this research is to provide a diagnostic tool to quickly identify diseases. This inexpensive, label free, high throughput technology allows the testing of several conditions simultaneously. This helps researchers understand the mechanism of binding and quantify the binding of biomolecules, which may enable the development of treatments for diseases involving membrane recruitment.

ACKNOWLEDGEMENTS

I would like to thank my committee chair, Dr. Hung-Jen Wu, and my committee members, Dr. M.M. Faruque Hasan, and Dr. Arul Jayaraman for their guidance and support throughout the course of this research.

I am also grateful to my lab mates Nolan, Joshua, Akshi and Chin-An who helped me through my research. I would also like to thank my friends, department faculty and staff for making my time at Texas A&M University a wonderful experience. Finally, thanks to my family for their constant support and encouragement.

NOMENCLATURE

CTB	Cholera Toxin B subunit
GM_1	Monosialoganglioside GM_1
GM_2	Monosialoganglioside GM_2
fGM_1	Fucosylated monosialoganglioside GM_1
LSPR	Localized surface plasmon resonance
GD_1b	Disialoganglioside GD_{1b}
aGM_1	Asialoganglioside GM_1
GM_3	Monosialoganglioside GM_3
LSPR	Localized surface plasmon resonance
MINLP	Mixed integer nonlinear programming
GM_1os	Monosialoganglisoside GM_1 oligosaccharide

TABLE OF CONTENTS

Page

LIST OF FIGURES

Page

LIST OF TABLES

Page

1. INTRODUCTION

Cholera is a virulent disease caused by consuming food or water contaminated with the bacterium known as *Vibrio cholerae*. [1] It causes an acute diarrheal infection and has caused several pandemics over many decades primarily due to lack of access to clean drinking water. Cholera not only poses a public health hazard but also lacks effective treatment. [2]

Other diseases which have recently affected a large population include Ebola and Zika virus epidemics, and treatment is largely symptomatic in these cases.[3-5] As these diseases resemble several others, like malaria and dengue respectively, it is often too late before any effective treatment may be administered. A common theme which may be observed among these diseases is that lives were lost primarily due to lack of access to proper diagnostic tools, lack of appropriate treatment methods and unavailability of qualified medical personnel. Clearly, there is a need to have an effective and inexpensive diagnostic tool, and a means to identify potential treatments in diseases involving membrane recruitment.

Many diseases involve biochemical processes that include binding between carbohydrates and biomolecules on the surface of cells. Glycan bound subunits may interact with neighboring binding domains thereby influencing the avidity with which it binds. Therefore, such cooperative binding can play a significant role in facilitating biochemical processes which in turn plays significant role in the propagation of diseases.

A nanocube sensor has been developed to quantify the binding between carbohydrates and biomolecules. A model system of cholera toxin has been studied here; to illustrate the use of this technology in understanding the role of cooperativity in binding of cholera toxin B (CTB) subunit with several gangliosides.

2. BACKGROUND*

2.1 Advantages of the nanocube system

Glycoarrays are currently used for glycan recognition and have glycans immobilized on a surface. [6] [7] Fluorescent labeling or immunostaining techniques can then be used to observe the amount of bound analyte. [8] However, this technology has many limitations. It is difficult to have multivalent binding in conventional glycoarrays, since the spacing and orientation of glycans cannot be properly controlled. These glycoarrays are typically used to study isolated glycans rather than several glycan structures and therefore it is difficult to obtain information on the binding cooperativities among glycans. Additionally, these glycoarrays offer little flexibility or ease of access and require special instrumentation to fabricate. One solution to this issue is to use fluidic bilayers where glycans may freely diffuse enabling them to organize themselves such that multivalent binding may be observed. [9, 10] However, this method also requires special equipment and the bilayers formed may not be stable for a long time. The nanocube sensor overcomes these problems and allows not only a fluidic bilayer but also label free detection and simple measurement requiring just a microplate reader.

---

*Parts of this section have been reprinted with permission from "Binding Cooperativity Matters: A GM_1-Like Ganglioside-Cholera Toxin B Subunit Binding Study Using a Nanocube-Based Lipid Bilayer Array" by Nolan C. Worstell, Pratik Krishnan, Joshua D. Weatherston, Hung-Jen Wu, 2016, PLoS ONE, 11(4), Copyright [2016] by Worstell et al. [11]

2.2 The nano-cube sensor

2.2.1 Silver nanocube synthesis

Silver nanocube sensors are synthesized using a previously established protocol known as the polyol method. [12] [13] This method involves the reduction of silver nitrate with pentane diol near its reflux temperature in the presence of poly(vinylpyrrolidone) as an agent to control the shape of the structure. The silver nanocubes formed are highly monodisperse and have an edge length of ~100 nm which can be confirmed by SEM. (Figure 1)

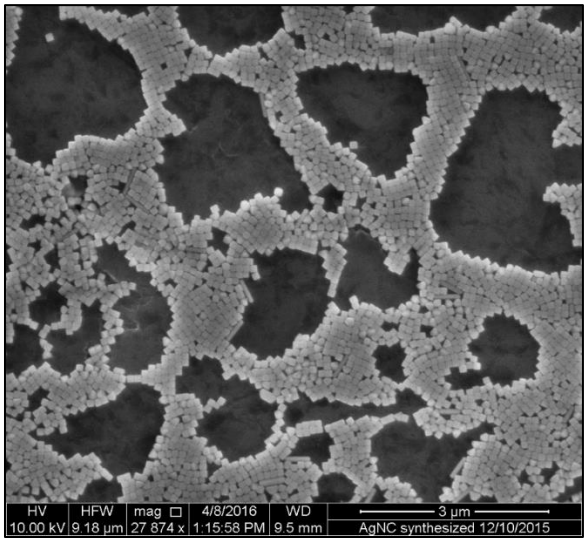

Figure 1. SEM image of a batch of silver nanocubes

2.2.1.1 Silver nanocube synthesis procedure

The nanocube synthesis procedure was taken from Tao et al. [12] . The procedure was based on the polyol method and described in brief as follows. First, 0.2 g of PVP was dissolved into 10 mL of PD. Next, 0.2 g of $AgNO_3$ was dissolved into 10 mL of PD with 30 μL of a 0.082 g/mL $CuCl_2$ in PD solution. Then, 20 mL of PD was heated in a 190°C silicon oil bath. After the PD was heated sufficiently, 500 μL of $AgNO_3$ solution and 500 μL of the PVP solution were added sequentially every minute. This was continued until all 10 mL of both the $AgNO_3$ and PVP solutions were added. When finished, the nanocubes were washed with 200 proof ethanol using a centrifuge.

2.2.2 Silica coating on the silver nanocube

A modified Stöber process is used to coat the nanocube with a thin layer of silica. [11] The silver nanocubes are first suspended in a 2-propanol. The solution is then mixed with water, tetraethyl ortho-silicate (TEOS) and ammonia. TEOS gets hydrolyzed to form silica which forms a thin layer on the surface of the silver nanocubes. Ammonia acts as a catalyst for the reaction. The thickness of the silica layer can be estimated using a TEM image of the nanocubes. (Figure 2) This silica coating allows the surface to be hydrophilic. This allows the silica coated cubes ($Ag@SiO_2$) to easily suspend in water and therefore, study binding in aqueous media.

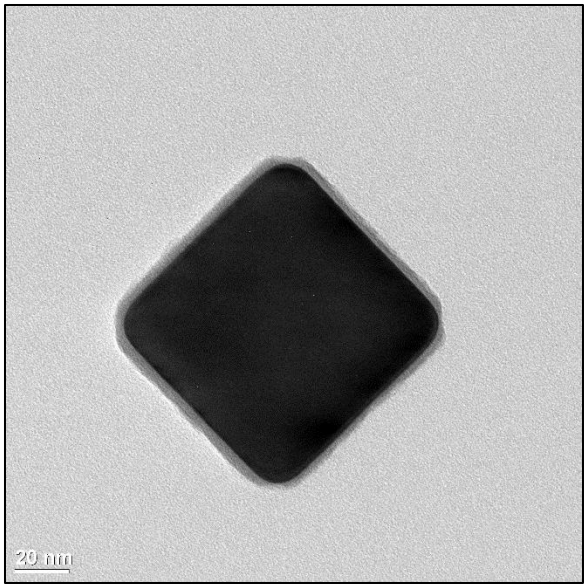

Figure 2. TEM image of a single cube from batch of silica coated cubes

2.2.2.1 Silica coating procedure

Our silica coating procedure was adapted from Wu et al. with few alterations and presented with alterations as follows. [13] To improve silica shell quality in the scaled-up synthesis batch, the silica coating reaction was conducted in 2-propanol, instead of ethanol. 20 mL of stock silver nanocube stored in ethanol was first transferred into 2-propanol. Then, the silver nanocube solution was suspended into 55 mL of 2-propanol and mixed with 22.1 mL of water, 6.80 mL of TEOS, and 3.4 mL of 0.84% ammonium hydroxide solution. Next, the solution was stirred at room temperature for 80 minutes. After the reaction finished, 50 mL of ethanol were added to quench the reaction. The

resultant particles were washed with Milli-Q® water a few times, and stored in Milli-Q® water for future use.

2.2.3 Extinction spectra of the silica coated nanocubes

The extinction (both absorption and scattering) spectrum of the silica-coated cubes ($Ag@SiO_2$) is observed using a standard UV-vis spectrophotometer. This spectrum includes the sharp quadrupolar localized surface plasmon resonance (LSPR) peak exhibited by the $Ag@SiO_2$ cubes. Silver nanocubes can have several spectral peaks and may have a substantial contribution from scattering as well. It should be noted that the field enhancement from the quadrupolar mode is higher than the dipole mode. [14]

2.2.4 Localized surface plasmon resonance

LSPR is the optical phenomenon generated when light interacts with conductive nanoparticles smaller than their wavelength. [15] It occurs when the frequency of movement of free electrons is nearly the same as the incident light. [16] Electric field of light collectively excites electrons in the conduction band resulting in coherent localized plasmon oscillations. [17] At a specific frequency of light, this collective oscillation results in a strong extinction of light. [18] This phenomenon is called localized surface plasmon resonance and the frequency at which this occurs is called as resonant frequency. This resonant frequency depends on several factors including the size, composition, geometry of the nanoparticle and the dielectric properties of the medium. [17]

2.2.5 Why silica coated silver nanocubes?

Silver is chosen for developing the sensor because it is a d-block element that exhibits localized surface plasmon resonance in the visible region of light. Silver also has the sharpest band energy gap and can exhibit better sensitivity than other metal nanoparticles. [19] Another crucial reason for using silver is because there is a well-established protocol to prepare a mono-disperse batch of nanocubes. [13] There have been semiconductors developed, which exhibit LSPR in the visible wavelength and may offer even sharper band energy gaps. [20] However, a protocol to prepare a highly mono-disperse batch of nanocubes has not yet been developed.

A cubic shape allows a uniform coating of the nanocubes and the corners of the cubes allow enhancement of the LSPR peak. [13] A highly irregular shape will allow enhancement, but a uniform supported lipid bilayer may not be coated. On the other hand, a spherical shape may allow uniform coating but will offer little field enhancement. Therefore, a cubic shape is optimally chosen.

Silica coating allows the surface to be hydrophilic in nature. This enables us to study protein binding in aqueous solutions and can also potentially increase the shelf life of silver nanocubes.

2.2.6 Supported lipid bilayer on the silica coated silver nanocubes

Supported lipid bilayers are coated on the surface of $Ag@SiO_2$. [11] Lipids of the required composition initially stored in chloroform or a mixture of chloroform, methanol and water are dried using a rotary evaporator. They are hydrated by adding water to get a

specific concentration of lipids. To attain small unilamellar vesicles (SUVs), the lipids are then extruded through filters or subjected to tip sonication. The SUVs are then coated on the silver nanocube using a modified vesicle fusion technique. It involves adding the cubes sequentially to the lipids while sonicating the solution in a bath sonicator. This ensures that the concentration of SUVs is always high and a lower amount of vesicles are needed as compared to the conventional vesicle fusion method. This fluidic supported lipid bilayer mimics the cell membrane and allows the lipids to have movements similar to those observed in the cell membrane. It can be observed on a cryo-TEM. (Figure 3)

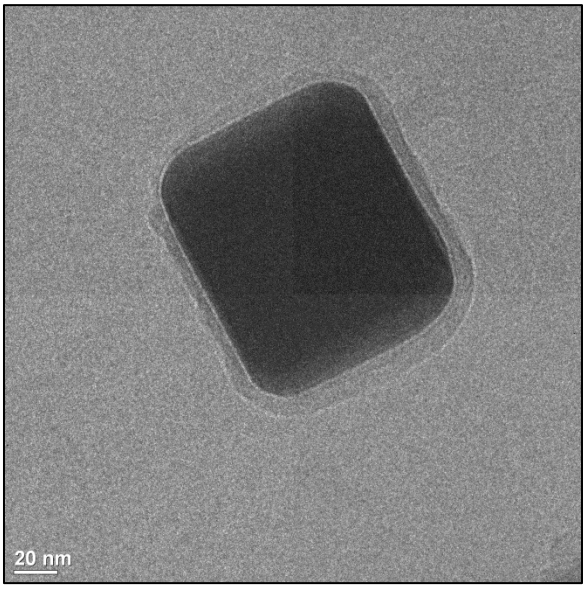

Figure 3. Cryo-TEM image showing the lipid bilayer coated on $Ag@SiO_2$ cubes [11]

2.2.6.1 Supported Bilayer Preparation

Small unilamellar vesicles (SUVs) were prepared as follows. The desired composition of lipids in chloroform was mixed and then dried using a rotary evaporator (Heidolph Hei-VAP Value®). Then, the dried lipids were rehydrated with Milli-Q® water and extruded through 100 nm polycarbonate filters (Whatman) using a Mini-extruder (Avanti Polar Lipids) or tip sonicated (Qsonica) to achieve an extruded lipid concentration of 3 mg/mL. Supported lipid bilayers were formed by a modified vesicle-fusion technique. In this technique, $Ag@SiO_2$ nanocubes were sequentially added into a SUV solution with a high SUV concentration in the initial coating solution. Briefly, 10 μL of nanocube solution and 30 μL of 2X TBS buffer were added to 20 μL of concentrated SUV solution (3 mg/mL) followed by 10 seconds of sonication in a bath sonicator (Branson). Then, 10 μL of nanocube solution and 10 μL of 2X TBS buffer were added followed by 10 seconds of sonication. This process was repeated until all of the nanocube solution had been added. After coating the supported bilayer, TBS buffer was added to the solution to reach the desired concentration of salt (1X TBS), SUV's, and nanocubes in the final solution.

2.2.7 Protein binding on the lipid bilayer coated $Ag@SiO_2$

Proteins can then be added to this lipid coated $Ag@SiO_2$ cubes. The amount of protein bound can be quantified by observing shifts in the location of the localized surface plasmon resonance (LSPR) peak in the extinction spectra of the lipid coated $Ag@SiO_2$ cubes. As proteins are organic molecules, the more they bind, the more they

alter the dielectric environment around the cubes. Since the LSPR peak is extremely sensitive to the dielectric environment, even small changes in the dielectric environment may be easily observed. [17]

Numerous biochemical processes begin through membrane recruitment and this tool can play a significant role in quantifying the binding of biomolecules and therefore serve as an effective diagnostic tool.

2.2.7.1 Protein binding measurement

Bilayer coated nanocubes were incubated with the desired protein concentration in a 384 well plate for 1.5 hours. Blank solutions were prepared for each CTB concentration by mixing buffer, SUVs, and CTB corresponding to that composition. Next, the 384 well plate was placed in a vacuum chamber at 40 cm Hg of vacuum for 15 minutes to remove air bubbles before collecting extinction spectra with a UV/Vis microplate spectrophotometer equipped with a CCD (FLUOstar Omega®, BMG-Labtech). The location of the quadrupole LSPR peak was detected by fitting a seventh order polynomial to the spectrum. The fitted spectrum resulted from averaging 200 flashes per well at a 1 nm spectral resolution; the scanning rate for each well was less than 1 second. All experiments were performed at room temperature.

The total amount of the CTB was calculated from the amount of CTB added. The amount of bound CTB was calculated from the observed LSPR shifts. The individual replicate LSPR shift was obtained by finding the wavelength corresponding to the maximum optical density given by the seventh order polynomial peak fitting. Then the

LSPR shifts of eight replicate wells were averaged to give the observed LSPR shift used to calculate the amount of bound CTB based on the Streptavidin-Biotin binding calibration. The difference between the total amount of CTB and the amount of bound CTB gave the amount of unbound CTB.

2.2.8 Calibration of silica coated silver nanocubes

2.2.8.1 Glycerol-Water test

Sensitivity of the silica coated silver nanocubes was determined by varying the dielectric environment of the cubes by placing them in solvents of known refractive indices. Mixtures of glycerol water were prepared and the $Ag@SiO_2$ cubes were suspended in them. The variation in the location of the localized surface plasmon resonance peak with change in refractive index was evaluated. (Figure 4)

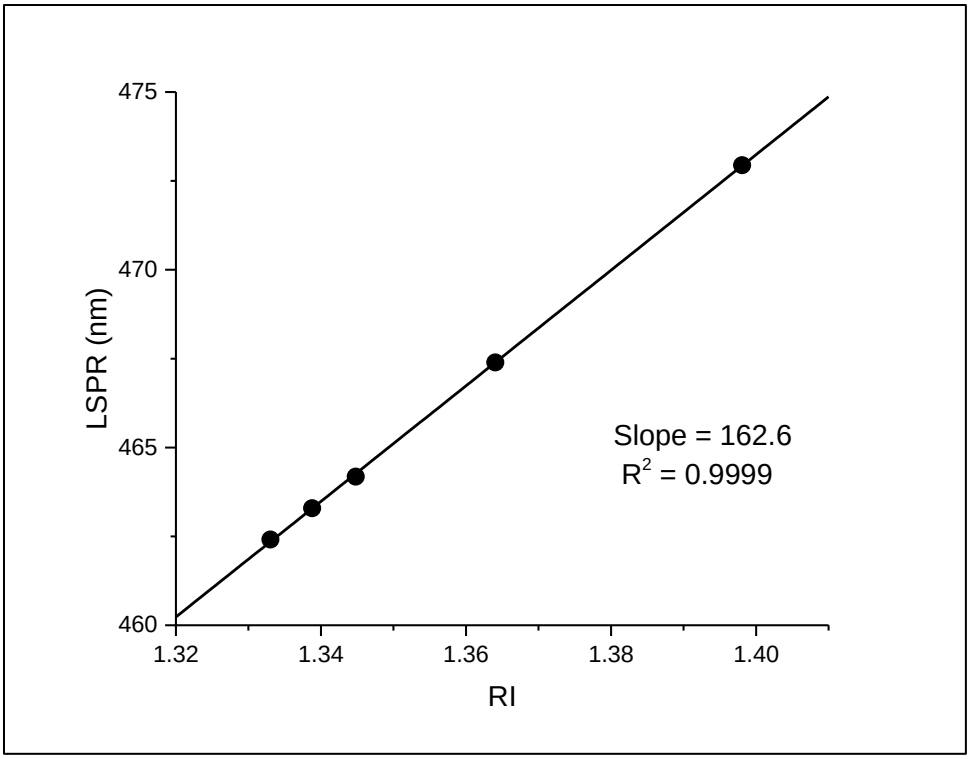

Figure 4. Glycerol water test results to estimate the sensitivity of cubes

2.2.8.2 Streptavidin-Biotin-DPPE calibration

The binding of streptavidin with Biotin-DPPE is very strong and therefore, may be assumed to be irreversible. Lipids with 1% biotin are prepared and a supported lipid bilayer was coated on the $Ag@SiO_2$ cubes. The binding with streptavidin allows the calibration of cubes by estimating the shifts in the localized surface plasmon peak as a function of protein density. (Figure 5) The surface density of streptavidin can be calculated by calculating the surface area of lipids assuming each lipid is DOPC. [11]

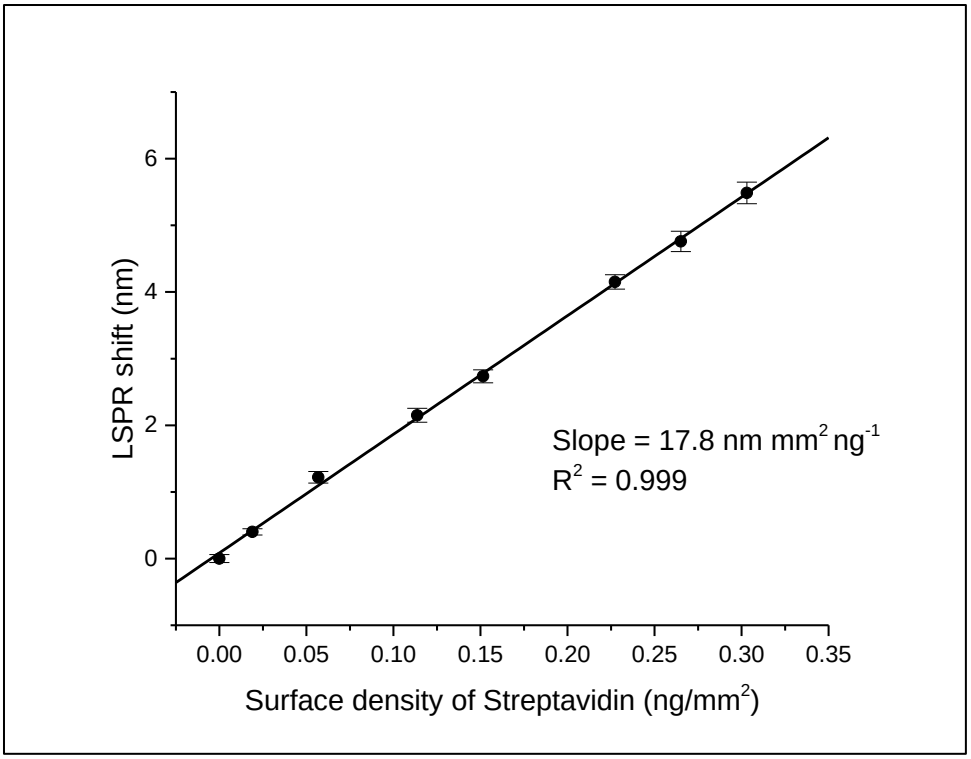

Figure 5. Streptavidin-Biotin-DPPE Calibration showing the variation of LSPR shift with surface density of Streptavidin [11]

2.2.8.3 CTB binding calculation

The amount of bound CTB is estimated by calculating shifts in the location of the LSPR peak and calculating protein density based on Streptavidin-Biotin calibration. The amount of unbound CTB is the difference between the total amount of CTB taken and the amount of bound CTB.

2.3 Cholera toxin

To study the application of our technology, the model system of cholera toxin was studied. Cholera toxin has two subunits, five B subunits which are responsible for the interaction of the toxin with the cell membrane and an A subunit which imparts virulence to the toxin. (Figure 6) [21] The presence of five binding sites makes the binding of CTB multivalent allowing the illustration of importance of cooperativity in multivalent binding.

It has been well-established in literature that cholera toxin binds with monosialoganglioside GM_1 (GM_1) found in the cell membrane of intestinal cells. [22] Once the B subunits bind with the GM_1, the toxin gets endocytosed by the cell. The A subunit gets activated and stimulates the adenylate cyclase, increasing the production of cyclic AMP levels. This activates the cystic fibrosis transmembrane conductance regulator which causes a sudden efflux of ions and water from the cell resulting in rice water like stool. This severe diarrhea may result in the death of an infected individual.

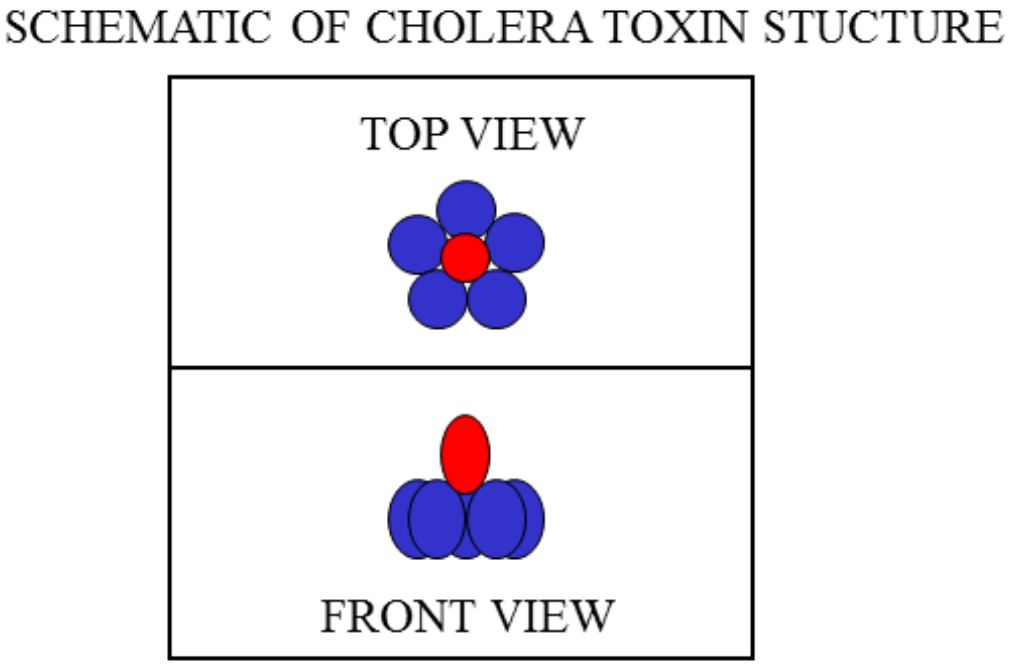

Figure 6. Schematic illustrating the structure of cholera toxin (The A subunit is shown in red while the B subunits are shown in blue) [23, 24]

3. CTB BINDING WITH GM1 *

The most obvious choice to study the binding of cholera toxin was GM_1 as the binding of CTB with GM_1 has been studied numerous times. [25-31] Therefore, the binding of cholera toxin with different compositions of GM_1 was studied. At a specific composition of lipid, the concentration of CTB was varied to obtain the equilibrium binding curve.

A semi empirical Hill-Waud model was fit through this data to obtain the dissociation constant, cooperativity and binding capacity, which have been explained below: [30]

$$\text{Hill Waud model}: \; C = C_{max} \times \frac{[P]^n}{K_h^n + [P]^n} \quad \ldots\ldots(1)$$

where, C_{max} is the binding capacity of the lipid bilayer, K_h is the apparent dissociation constant and n is the coefficient of cooperativity and are obtained by fitting experimental data with the above model. C is the concentration of the bound CTB while P is the concentration of the unbound CTB. P is obtained by subtracting the concentration of the bound CTB from total CTB added. The concentration of total CTB is predetermined while C is obtained through experiments.

*Reprinted with permission from "Binding Cooperativity Matters: A GM_1-Like Ganglioside-Cholera Toxin B Subunit Binding Study Using a Nanocube-Based Lipid Bilayer Array" by Nolan C. Worstell, Pratik Krishnan, Joshua D. Weatherston, Hung-Jen Wu, 2016, PLoS ONE, 11(4), Copyright [2016] by Worstell et al. [11]

An n value greater than 1 implies positive cooperativity while a value less than 1 implies negative cooperativity. The physical significance of the n value is that it highlights whether one binding favors or hinders subsequent binding. If it favors further binding, it is greater than 1; else it is less than 1.

Several different compositions of GM_1 were taken including 1, 2, 4 and 10 mol%. (Figure 7) On increasing the mol% of GM_1 in the lipid bilayer, the binding capacity increased. The dissociation constant was also found to increase with increasing mol% of GM_1. The n value in all cases was found to be greater than 1, indicating positive cooperativity. (Table 1) Therefore, as one GM_1 binds, it favors further binding. These results match those obtained by Shi et al. [30]

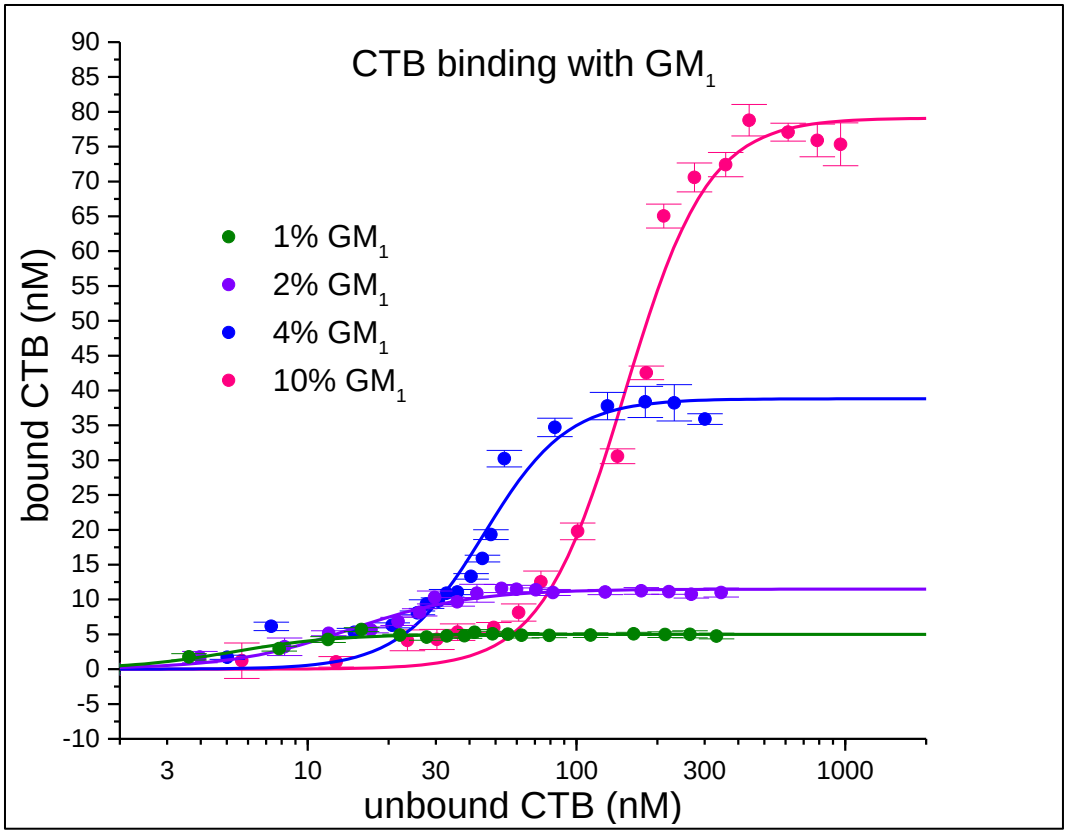

Figure 7. Binding curves for CTB binding with GM_1 (1, 2, 4 and 10 mol %)

Table 1. Fitted parameters using Hill's Equation for 1, 2, 4 and 10 mol % GM_1

GM_1 %	K_h (nM)	C_{max} (nM)	n	R^2
1	5.6 ± 0.6	5.3 ± 0.1	2.25 ± 0.45	0.943
2	14.5 ± 1.0	11.5 ± 0.3	1.93 ± 0.25	0.968
4	48.0 ± 3.0	41.0 ± 1.8	2.79 ± 0.45	0.959
10	151.0 ± 7.0	79.0 ± 2.3	2.79 ± 0.31	0.986

4. CTB BINDING WITH LIGANDS OTHER THAN GM_1 *

Beyond GM_1, other GM_1-like gangliosides associated with CTB have been identified. Most of the previous studies identified GM_1- and GM_1-like ganglioside-CTB binding avidities with isothermal titration calorimetry (ITC), mass spectrometry (MS), or immobilized receptors on solid substrates. [26, 29, 32-35] Some studies conducted the CTB-ganglioside binding measurements using fluidic lipid bilayers. [29, 31, 36-39] Regardless of measurement technique, these studies often reported the apparent association constants and thermodynamic parameters of CTB binding to various gangliosides, but few of them analyzed the cooperative actions between bound gangliosides. In the past, CTB has been used to quantify the amount of GM_1 that was present in a cell membrane [40, 41] , but the validity of this approach was refuted by Yanagisawa et al. [42] In the absence of GM_1, Yanagisawa et al. observed strong reactivity between CTB and embryonic neuroepithelial cells and attributed this phenomenon to the expression of GM_1- like ganglioside. To further investigate cooperative interaction in multivalent CTB binding to GM_1-like gangliosides, two gangliosides, fucosyl-GM_1 and GM_2, were selected, which exhibit mild and weak binding avidity to CTB, respectively. At a specific composition of lipids in the bilayer (2 mol %), the binding curves of three gangliosides, GM_1, GM_2 and fGM_1 were compared. (Figure 8)

---

*Reprinted with permission from "Binding Cooperativity Matters: A GM_1-Like Ganglioside-Cholera Toxin B Subunit Binding Study Using a Nanocube-Based Lipid Bilayer Array" by Nolan C. Worstell, Pratik Krishnan, Joshua D. Weatherston, Hung-Jen Wu, 2016, PLoS ONE, 11(4), Copyright [2016] by Worstell et al. [11]

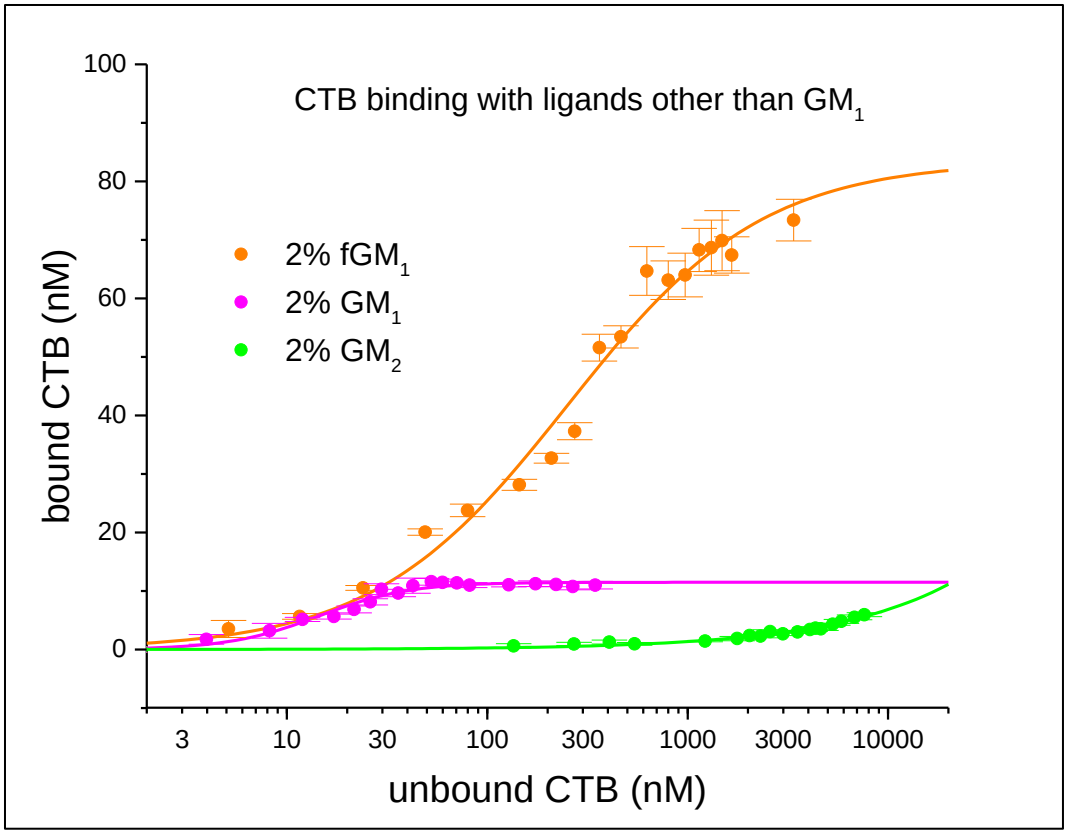

Figure 8. Binding curves for CTB binding with 2 mol % GM_1, fGM_1 and GM_2

The Hill-Waud model was also fit to the experimental data to estimate K_h , C_{max} and n. (Table 2) K_h was found to be at least an order of magnitude higher for fGM_1. In the case of GM_2, it was not possible to estimate the K_h or C_{max} with accuracy as it wasn't possible to reach the plateau region of the binding curve, which lay beyond physiologically relevant concentrations of CTB.

The n value could be determined for both cases and was found to be less than 1 highlighting that their binding is negatively cooperative. One surprising observation was

that the C_{max} value was greater for fGM_1 than GM_1 even though it has a lower binding avidity for CTB (illustrated by its higher K_h value).

Table 2. Fitted parameters using Hill's Equation for 2 mol % GM_1, fGM_1 and GM_2

mol % of Lipid			**Hill's Equation fitting parameters**			
GM_1 %	**fGM_1 %**	**GM_2 %**	**K_h (nM)**	**C_{max} (nM)**	**n**	**R^2**
0	**2**	**0**	251.8 ± 47.1	83.5 ± 5.3	0.89 ± 0.10	0.985
2	**0**	**0**	14.5 ± 1.0	11.5 ± 0.3	1.93 ± 0.25	0.968
0	**0**	**2**	$(1.661 \pm \text{n/a}) \cdot 10^{8*}$	$(6.39 \pm 2.91) \cdot 10^{3*}$	0.70 ± 0.04	0.971^{*}

*The value ± S.E. of the estimate given is highly uncertain since plateau region was not reached

The higher C_{max} value may be explained through the change in cooperativity. Binding capacity increases for negatively cooperative ligands because negative cooperativity hinders subsequent binding. Therefore, for a given number of ligands, the number of CTB pentamers with which they bind is higher since fewer sites are occupied. In the case of positively cooperative ligands, more sites are occupied as subsequent binding is favored which implies they bind with fewer CTB pentamers.

To ensure that the degradation of GM_1 did not cause unexpected lower binding capacity, the quality of GM_1 was also verified by testing GM_1 from three different vendors (Avanti, Matreya and Sigma). All three were found to be similar. (Figure 9)

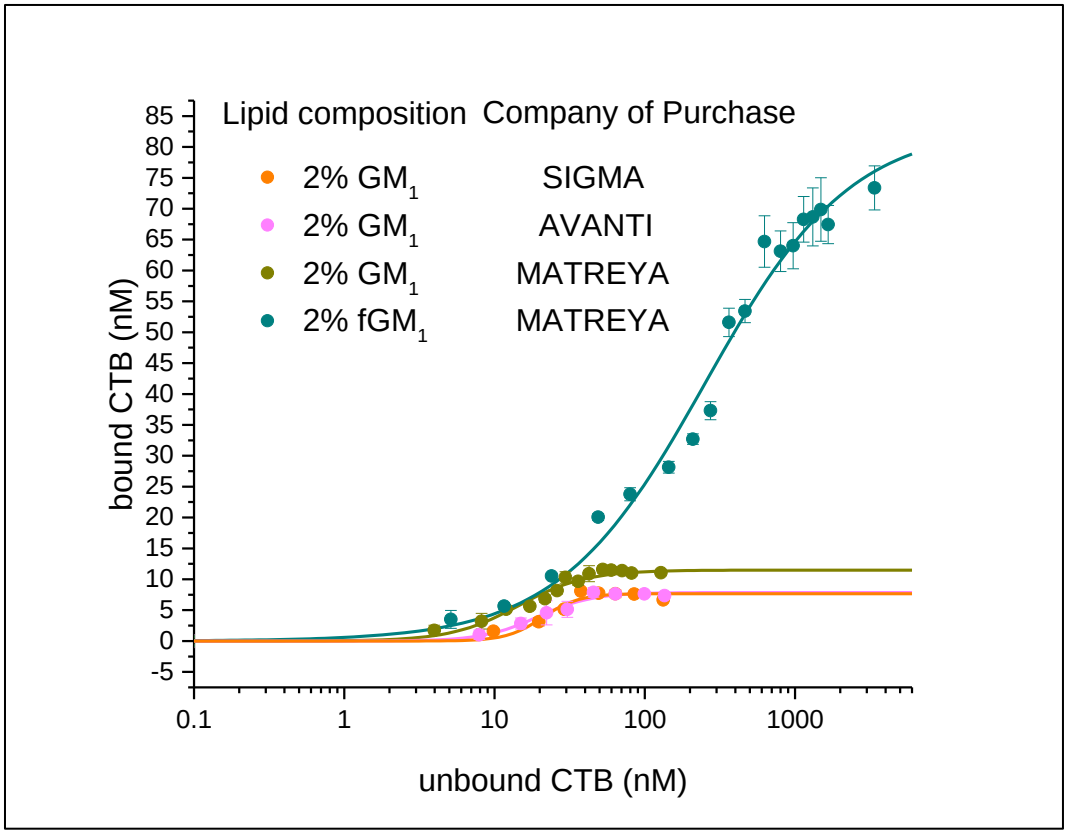

Figure 9. Binding curves for CTB binding with 2 mol % GM_1 from three different vendors [11]

5. CTB BINDING WITH fGM_1 *

Several different compositions of fGM_1 were also studied to verify if it is negatively cooperative for different compositions.

On obtaining binding curves for 0.5, 1, 1.5 and 2%, it could be observed that on increasing the mol% of fGM_1, the binding capacity increased just like what was observed for GM_1. (Figure 10) The K_h value was also found to increase with increasing mol% of fGM_1. The n value in all cases was found to be either less than 1 or close to 1 indicating negatively cooperative or non-cooperative binding. (Table 3)

Table 3. Fitted parameters using Hill's Equation for fGM_1 (0.5, 1, 1.5 and 2 mol %)

Lipid composition (mol %)	**Hill's Equation fitting parameters**			
fGM_1 %	**K_h (nM)**	**C_{max} (nM)**	**n**	**R^2**
0.5	59.4 ± 5.7	12.0 ± 0.3	0.78 ± 0.05	0.993
1	270.8 ± 56.8	32.5 ± 1.9	0.69 ± 0.06	0.992
1.5	129.1 ± 13.0	34.4 ± 1.1	1.06 ± 0.09	0.989
2	251.8 ± 47.1	83.5 ± 5.3	0.89 ± 0.10	0.985

*Reprinted with permission from "Binding Cooperativity Matters: A GM_1-Like Ganglioside-Cholera Toxin B Subunit Binding Study Using a Nanocube-Based Lipid Bilayer Array" by Nolan C. Worstell, Pratik Krishnan, Joshua D. Weatherston, Hung-Jen Wu, 2016, PLoS ONE, 11(4), Copyright [2016] by Worstell et al. [11]

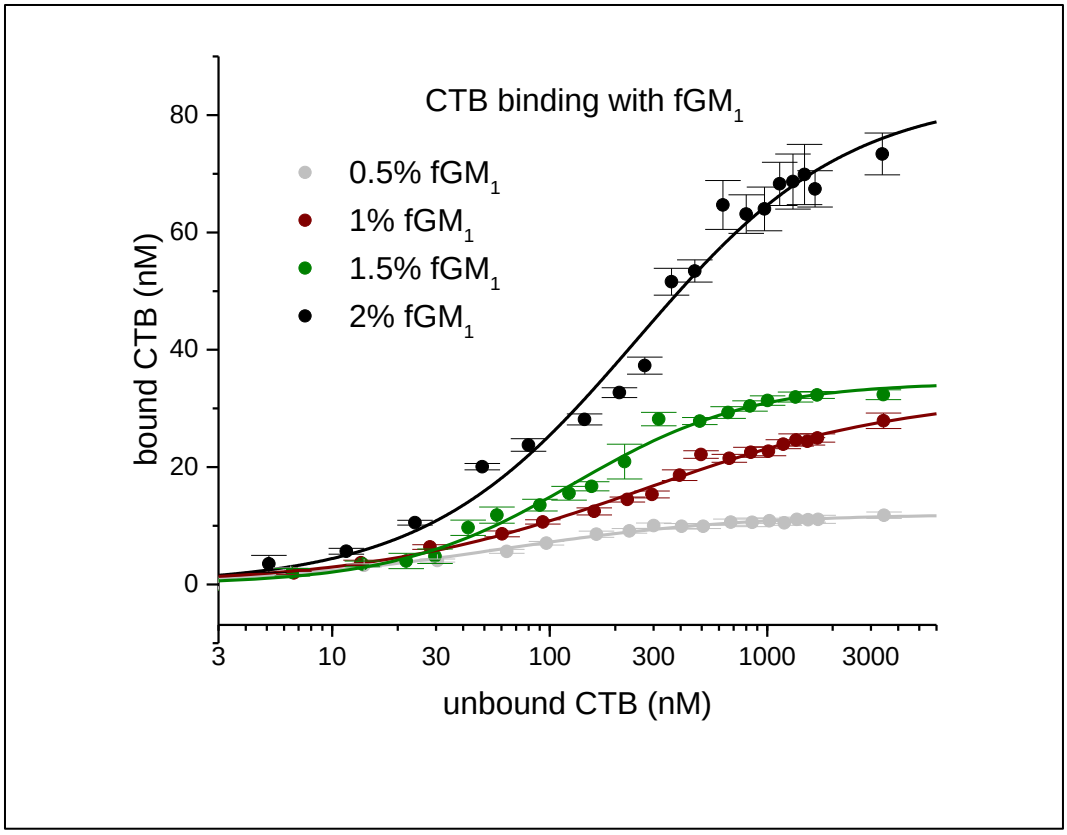

Figure 10. Binding curves for CTB binding with fGM_1 (0.5, 1, 1.5 and 2 mol %)

6. CTB BINDING WITH MIXTURES OF fGM_1 AND GM_2 *

Mixtures of fGM_1 and GM_2 were also studied to understand how one ligand can influence the binding of another (both are negatively cooperative ligands). Keeping the total ligand composition as 2 mol%, different amounts of fGM_1 and GM_2 were taken as follows: 0.5 mol% fGM_1 + 1.5 mol% GM_2, 0.75 mol% fGM_1 + 1.25 mol% GM_2, 1 mol% fGM_1 + 1 mol% GM_2 and 1.5 mol% fGM_1 + 0.5 mol% GM_2. Binding curves were made for all cases and the Hill-Waud model was fit to the experimental data. (Table 4) As the Hill-Waud model assumes single receptor binding, the parameters obtained from the fitting lack physical significance for mixtures.

Table 4. Fitted parameters using Hill's Equation for mixtures of fGM_1 and GM_2

Lipid composition (mol %)		**Hill's Equation fitting parameters**			
fGM_1 %	**GM_2 %**	**K_h (nM)**	**C_{max} (nM)**	**n**	**R^2**
0.5	**1.5**	563.4 ± 156.4	88.7 ± 8.5	0.85 ± 0.11	0.982
0.75	**1.25**	380.4 ± 159.1	91.0 ± 9.1	0.56 ± 0.07	0.978
1	**1**	830.5 ±114.6	96.6 ±4.9	0.82 ±0.04	0.998
1.5	**0.5**	682.7 ± 190.5	92.6 ± 7.9	0.69 ± 0.05	0.993

*Reprinted with permission from "Binding Cooperativity Matters: A GM_1-Like Ganglioside-Cholera Toxin B Subunit Binding Study Using a Nanocube-Based Lipid Bilayer Array" by Nolan C. Worstell, Pratik Krishnan, Joshua D. Weatherston, Hung-Jen Wu, 2016, PLoS ONE, 11(4), Copyright [2016] by Worstell et al. [11]

Surprisingly, at the highest concentration of free CTB tested (3.4 μM), amount of CTB bound was similar to 2 mol% fGM_1. (Figure 11) This implied that GM_2 was able to bind with CTB in the presence of fGM_1 and compensated for the reduced concentration of fGM_1. If the binding of fGM_1 and GM_2 were independent of each other, the binding capacity in each case would be different. However, this is not observed and highlights that heterogeneous mixtures of ligands may bind differently than if only pure components were present. This illustrates how weak binding ligands may have a significantly enhanced binding capacity in the presence of other stronger binding ligands.

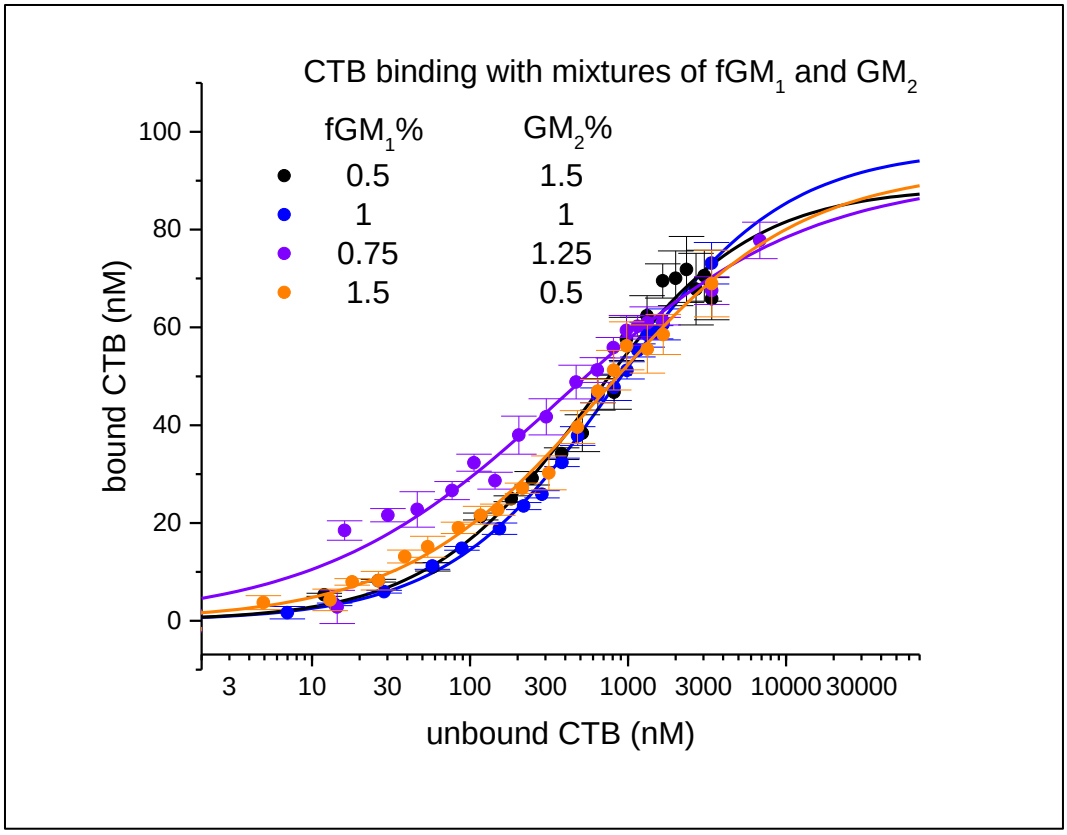

Figure 11. Binding curves for CTB binding with mixtures of fGM_1 and GM_2

7. CTB BINDING WITH CONTROL *

A control of 90% DOPC and 10% DOPS was taken to ensure there is no non-specific binding of CTB with the lipid bilayer. (Figure 12) There was negligible binding observed highlighting the absence of non-specific binding.

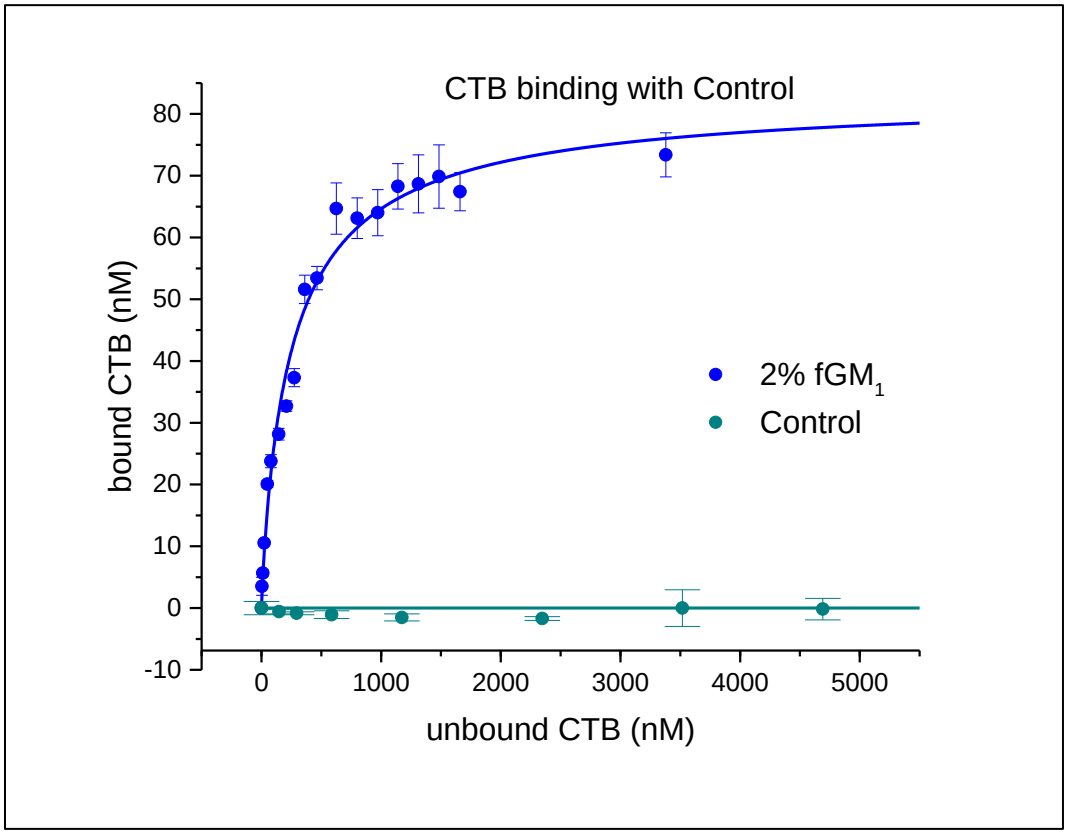

Figure 12. Binding curves for CTB binding with control

*Reprinted with permission from "Binding Cooperativity Matters: A GM_1-Like Ganglioside-Cholera Toxin B Subunit Binding Study Using a Nanocube-Based Lipid Bilayer Array" by Nolan C. Worstell, Pratik Krishnan, Joshua D. Weatherston, Hung-Jen Wu, 2016, PLoS ONE, 11(4), Copyright [2016] by Worstell et al. [11]

8. THEORETICAL MODEL TO STUDY THE INFLUENCE OF COOPERATIVITY ON BINDING CAPACITY *

To elucidate the surprisingly higher binding capacity observed for fGM_1, a stepwise binding model was adapted from Klassen and his coworkers. (Figure 13) [43] They used direct electrospray ionization mass spectrometry to estimate binding constants for different states observed in their model. They considered the influence of either one or both adjacent sites being occupied by GM_1 ligands and used three apparent binding constants to describe reaction paths to all possible states.

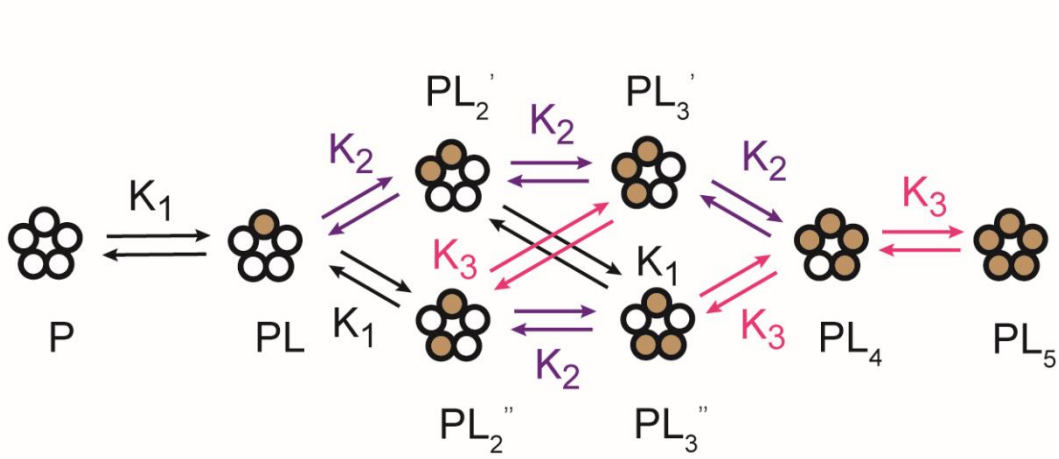

Figure 13. Stepwise binding model adapted from Klassen and his coworkers [11] [43]

*Reprinted with permission from "Binding Cooperativity Matters: A GM_1-Like Ganglioside-Cholera Toxin B Subunit Binding Study Using a Nanocube-Based Lipid Bilayer Array" by Nolan C. Worstell, Pratik Krishnan, Joshua D. Weatherston, Hung-Jen Wu, 2016, PLoS ONE, 11(4), Copyright [2016] by Worstell et al. [11]

Writing the material balance for a CTB pentamer (P),

$\mathbf{P_T} = [\mathbf{P}] + [\mathbf{PL}] + [\mathbf{PL_2'}] + [\mathbf{PL_2''}] + [\mathbf{PL_3'}] + [\mathbf{PL_3''}] + [\mathbf{PL_4}] + [\mathbf{PL_5}]$…… (2)

where P_T is the total concentration of CTB, [P] is the concentration of free CTB, and $[PL]/[PL_2]/[PL_3]/[PL_4]/[PL_5]$ are the protein-ligand binding complexes with 1, 2, 3, 4, and 5 ligands respectively

Writing material balance for the ligand L,

$\mathbf{L_T} = [\mathbf{L}] + [\mathbf{PL}] + \mathbf{2} \times ([\mathbf{PL_2'}] + [\mathbf{PL_2''}]) + \mathbf{3} \times ([\mathbf{PL_3'}] + [\mathbf{PL_3''}]) + \mathbf{4} \times [\mathbf{PL_4}] + \mathbf{5} \times [\mathbf{PL_5}]$…… (3)

where L_T is the total concentration of ligands and L is concentration of unbound ligands.

At equilibrium, each reaction species have material balances as follows:

$[\mathbf{PL}] = \mathbf{5} \times \mathbf{K_1}[\mathbf{P}][\mathbf{L}]$…….. (4)

$[\mathbf{PL_2'}] = [\mathbf{PL}][\mathbf{L}] = \mathbf{5} \times \mathbf{K_1K_2}[\mathbf{P}][\mathbf{L}]^2$ ……..…….....(5)

$[\mathbf{PL_3'}] = [\mathbf{PL_2'}][\mathbf{L}] = \mathbf{5} \times \mathbf{K_1K_2}^2[\mathbf{P}][\mathbf{L}]^3$…….....(6)

$[\mathbf{PL_4}] = [\mathbf{PL_3'}][\mathbf{L}] = \mathbf{5} \times \mathbf{K_1K_2}^3[\mathbf{P}][\mathbf{L}]^4$ ……...……(7)

$[\mathbf{PL_5}] = \mathbf{K_3}^5[\mathbf{PL_4}][\mathbf{L}] = \mathbf{K_1K_2}^3\mathbf{K_3}[\mathbf{P}][\mathbf{L}]^5$ ……(8)

$[\mathbf{PL_2''}] = [\mathbf{PL}][\mathbf{L}] = \mathbf{5} \times \mathbf{K_1}^2[\mathbf{P}][\mathbf{L}]^2$ ……..……(9)

$[\mathbf{PL_3''}] = [\mathbf{PL_2''}][\mathbf{L}] = \mathbf{5} \times \mathbf{K_1}^2\mathbf{K_2}[\mathbf{P}][\mathbf{L}]^3$……..…… ...(10)

2 and 3 can be written as:

$\mathbf{P_T} = [\mathbf{P}] + \mathbf{5} \times \mathbf{K_1}[\mathbf{P}][\mathbf{L}] + \mathbf{5} \times \mathbf{K_1K_2}[\mathbf{P}][\mathbf{L}]^2 + \mathbf{5} \times \mathbf{K_1}^2[\mathbf{P}][\mathbf{L}]^2 + \mathbf{5} \times \mathbf{K_1K_2}^2[\mathbf{P}][\mathbf{L}]^3 + \mathbf{5} \times \mathbf{K_1}^2\mathbf{K_2}[\mathbf{P}][\mathbf{L}]^3 + \mathbf{5} \times \mathbf{K_1K_2}^3[\mathbf{P}][\mathbf{L}]^4 + \mathbf{K_1K_2}^3\mathbf{K_3}[\mathbf{P}][\mathbf{L}]^5$ ……..(11)

$$\mathbf{L_T = L + 5 \times K_1[P][L] + 2 \times (5 \times K_1K_2[P][L]^2 + 5 \times K_2^2[P][L]^2) + 3 \times (5 \times K_1K_2^2[P][L]^3 + 5 \times K_1^2K_2[P][L]^3) + 4 \times (5 \times K_1K_2^3[P][L]^4) + 5 \times K_1K_2^3K_3[P][L]^5} \quad \text{……(12)}$$

The values for K_1, K_2, and K_3 for CTB binding with GM_1 are 3.2 x 10^6 M^{-1}, 5.5 x 10^6 M^{-1}, and 9.5 x 10^6 M^{-1} respectively. Considering cooperative interactions, K_2 and K_3 are multiplied by a factor 'α'. Therefore,

$$\boldsymbol{K_2 = \alpha \times K_1} \quad \text{……...…(13)}$$

$$\boldsymbol{K_3 = \alpha^2 \times K_1} \quad \text{……..(14)}$$

α is around 2 when GM_1 is the binding receptor. α less than 1 implies negatively cooperative binding. Choosing an arbitrary α less than 1 (to represent fGM_1 and GM_2), we take α = 0.5. The value of L_T was taken to be 1 μM and P was varied from 0.1 nM to 1 μM. L was then estimated from (12). $P_T - P$ gives the amount of bound CTB.

A plot of unbound vs. bound CTB for the two cases shows how the binding capacity is higher if the ligand is negatively cooperative. (Figure 14) The K_1 value was also reduced to reflect the lowered avidity of fGM1 for CTB and the results were still consistent. This proved the experimental results were indeed correct.

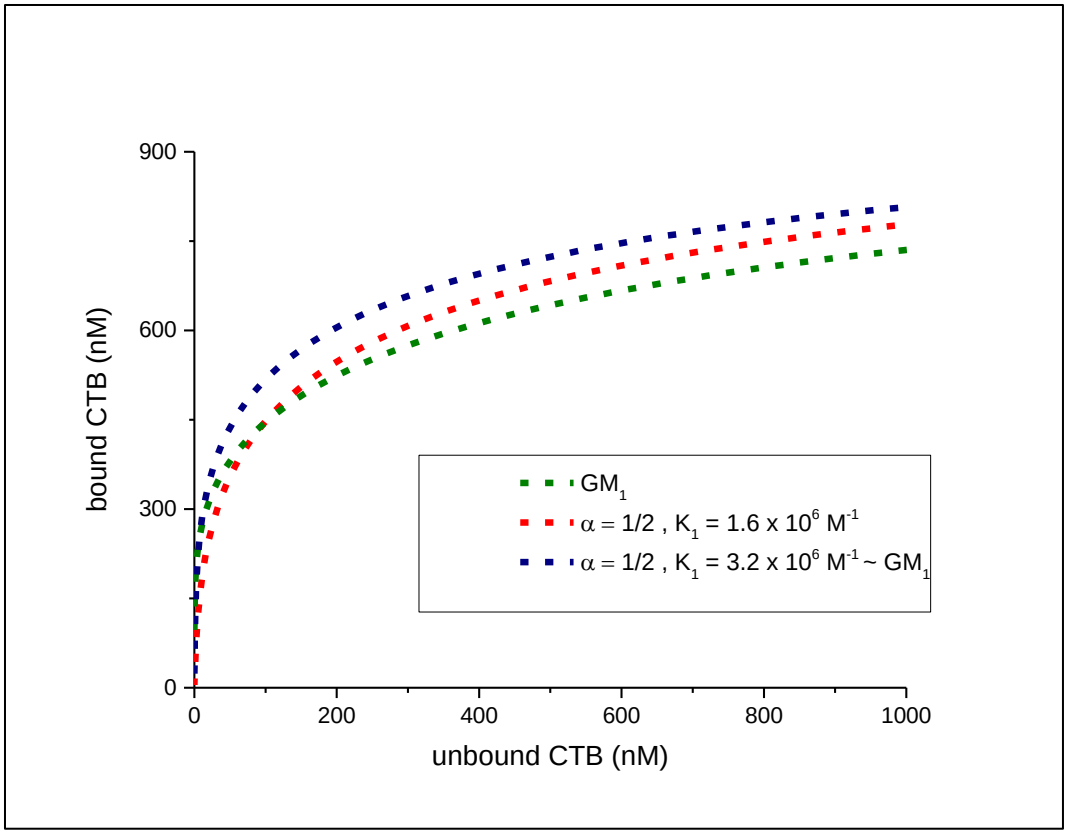

Figure 14. Simulated binding curves based on the stepwise binding model for CTB binding with GM_1 and a negatively cooperative ligand ($\alpha = 1/2$) with same K_1 and a lowered K_1

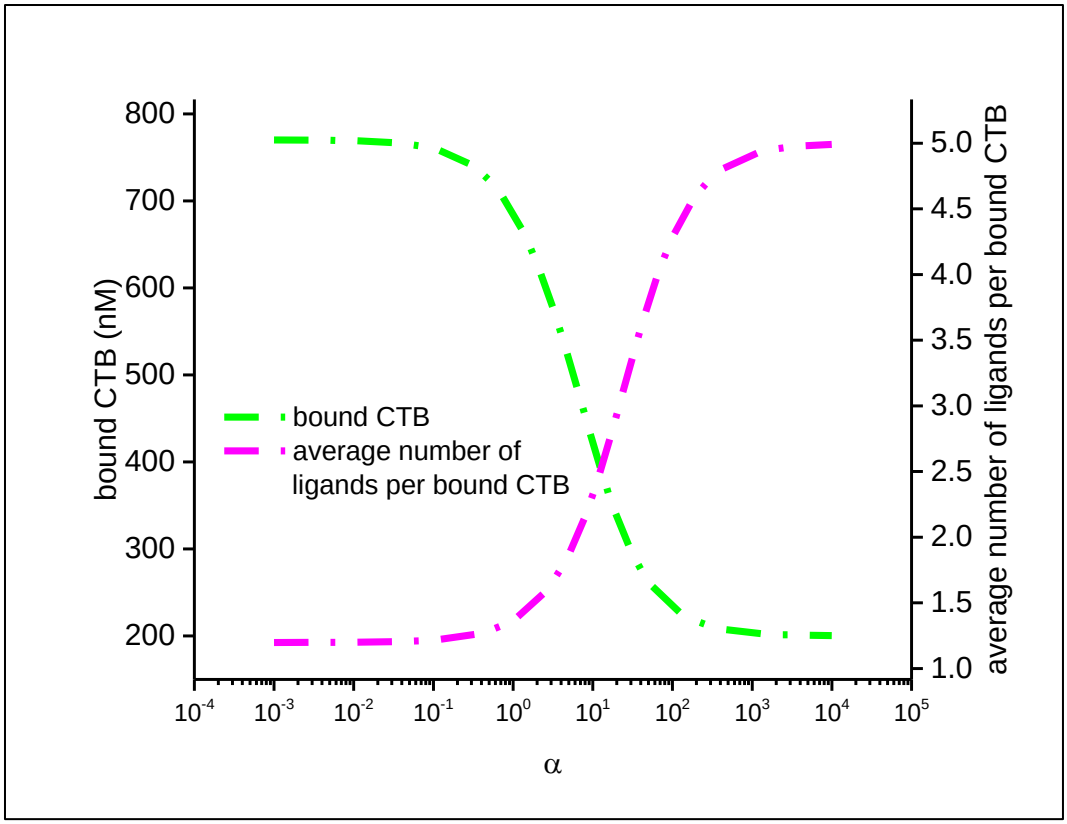

Figure 15. Simulated binding curves based on the stepwise binding model for CTB binding with ligands by varying cooperativity at a fixed unbound CTB concentration (500 nM)

Positive cooperativity favored higher binding states and limited the number of ligands available to bind to CTB resulting in a lower binding capacity as compared to negatively cooperative binding. It is clear from Figure 15, that increasing cooperativity increases the number of ligands bound per CTB.

Thus, this theoretical model provided an understanding of how negatively cooperative ligands may exhibit higher binding capacity even though they may have lower avidity.

9. GLYCOARRAY TO STUDY HETEROGENEOUS BINDING COOPERATIVITY

It has been demonstrated that the weak binding ligand (GM_2) was activated by strong binding ligand (fGM_1) resulting in higher binding capacity. The binding of CTB with two different gangliosides, fGM_1 and GM_2 were investigated previously. Some researchers have claimed that CTB may bind with other GM_1-like glycolipids, such as GD_1b, aGM_1 and possibly GM_3. (Figure 16) [25, 27, 31] The positive binding cooperativity among these ligands may alter the CTB binding capacities on heterogeneous cell surfaces.

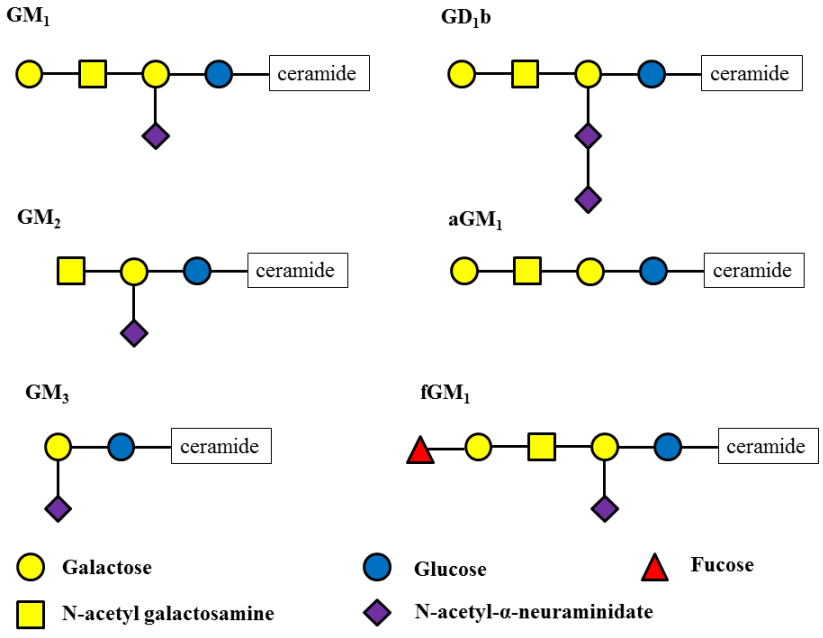

Figure 16. Schematic highlighting the sugar groups in the relevant gangliosides [44]

To understand the influences of heterogeneous binding cooperativity, a glycoarray was constructed with these ligands and different combinations of these ligands were studied. (Table 5) This allowed the understanding of enhancement in binding for mixtures and the study of the influence of structures of gangliosides in binding with CTB. The gangliosides considered for this glycoarray include: GM_1, GM_2, fGM_1, GD_1b and GM_3.

Table 5. Glycoarray of several ligands

	GM_1	GM_2	GM_3	fGM_1	GD_1b
GM_1					
GM_2					
GM_3					
fGM_1					
GD_1b					

The preliminary data obtained have been shown here. For pure components 1 mol % was taken and the entire binding curve was obtained. (Figure 17) Binary mixtures were considered and each component had a composition of 1 mol %. For these, two points at higher CTB concentrations (706 nM and 1726 nM) were considered so as to illustrate how binding capacity varies for different ligand compositions.

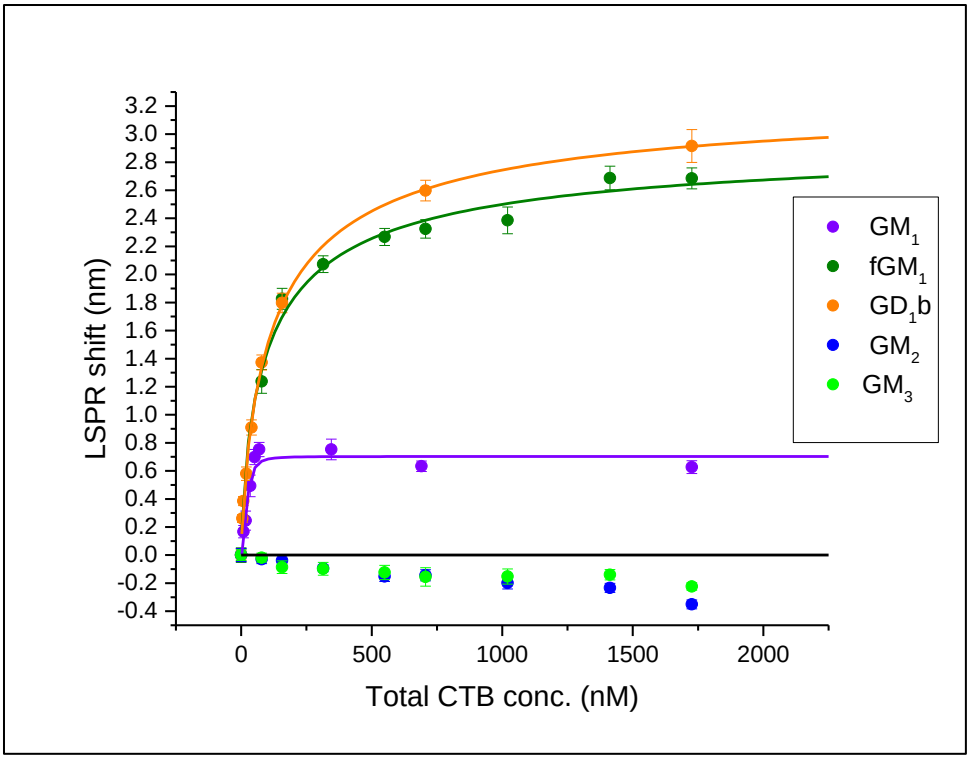

Figure 17. Pure component binding data for ligands used in the glycoarray

To study enhancement in binding for mixtures, heterogeneous cooperativity was defined as follows:

$$\text{Heterogeneous cooperativity} = \phi = \frac{\text{Amount of CTB bound to the mixture}}{\text{Sum of the amount of CTB bound to individual components}}$$

For a binary mixture, binding cooperativity can be defined as:

$$\text{Cooperativity} = [PAB]/([PA] + [PB])$$

where [PA], [PB] and [PAB] is the amount of bound CTB to gangliosides A, B and combination of both A and B respectively. If the cooperativity is greater than 1, then it implies the gangliosides are positively cooperative. If it is less than 1, then the

gangliosides are negatively cooperative. A concentration of 1% is chosen so as to minimize the effect of steric hindrance [45] [46] and to prevent a heterogeneous distribution of the gangliosides [30] [47].

It is clear from the results obtained that some mixtures exhibit cooperativity in binding. (Table 6 and Table 7) Some of the mixture pairs that seemed to exhibit significant positive cooperativity were:

1. GM_1 +GM_2
2. fGM_1+GM_2
3. GD_1b+GM_2
4. GD_1b+GM_3

More statistical analysis into the data collected may highlight in which cases the cooperativity is significant. It is likely that fGM_1+ GM_3 also exhibits positive cooperative, but more experiments need to be conducted before that may be concluded. It should be noted that for GM_2 and GM_3, the binding was taken to be zero since no significant binding was observed in either case. Also, for the combination of GM_2 and GM_3, no significant binding was observed. Therefore, for this case cooperativity was taken as 1.

Table 6. CTB binding with different ligands at a total CTB concentration of 706 nM, green highlights positive cooperativity (>1.5)

	GM_1	fGM_1	GD_1b	GM_2	GM_3
GM_1	1.0	1.1	0.9	1.5	1.2
fGM_1		1.0	0.9	1.6	1.2
GD_1b			1.0	2.3	2.1
GM_2				1.0	1.0
GM_3					1.0

Table 7. CTB binding with different ligands at a total CTB concentration of 1726 nM, green highlights positive cooperativity (>1.5)

	GM_1	fGM_1	GD_1b	GM_2	GM_3
GM_1	1.0	1.1	1.1	2.2	1.0
fGM_1		1.0	1.1	1.5	1.1
GD_1b			1.0	2.2	2.0
GM_2				1.0	1.0
GM_3					1.0

10. NO ENHANCEMENT OF BINDING IN MIXTURES OF OLIGOSACCHARIDE GM_1 AND GLYCOLIPID GM_2

To verify the cause of binding enhancement, GM_1 oligosaccharide (GM_1os) sugar were purchased and pre-bound to CTB. Ag@SiO_2 nanocubes were then coated with a lipid bilayer having 2% GM_1 and 2% GM_2.The binding capacity at a total CTB concentration of 706 nM was measured while varying the sugar concentration. In the case of 2% GM_1, the binding capacity was found to decrease with increase in sugar concentration. This is because as more CTB binds to GM_1os, the lesser number will bind with the lipid bilayer on the Ag@SiO_2 nanocubes. In the case of 2% GM_2, negligible binding was observed. This allows us to hypothesize that it is probably not the allosteric effect causing an enhancement in binding. This is because if allosteric effects were involved, the pre-bound CTB (with GM_1os) would have avidity for the nanocubes and exhibit higher binding, which was not the case. The enhancement may be explained by understanding the mechanism of binding. It is possible that when both GM_1 and GM_2 are present simultaneously in the bilayer, the CTB binds first to the GM_1 for which it has a high avidity. Now that one site on the CTB is bound to GM_1, the remaining bindings will be two dimensional rather than the conventional three dimensional binding. But a reduction in dimensionality increases the rate of binding and the effective concentration of the ligands.[48-50] The time for searching new ligands to bind with is significantly lowered. In two dimensions, the concentration of ligands depends on the surface area rather than volume and also gets significantly affected. Therefore, it can be hypothesized

that the higher effective concentration of GM_2 allows it to contribute to the binding resulting in an enhanced binding capacity.

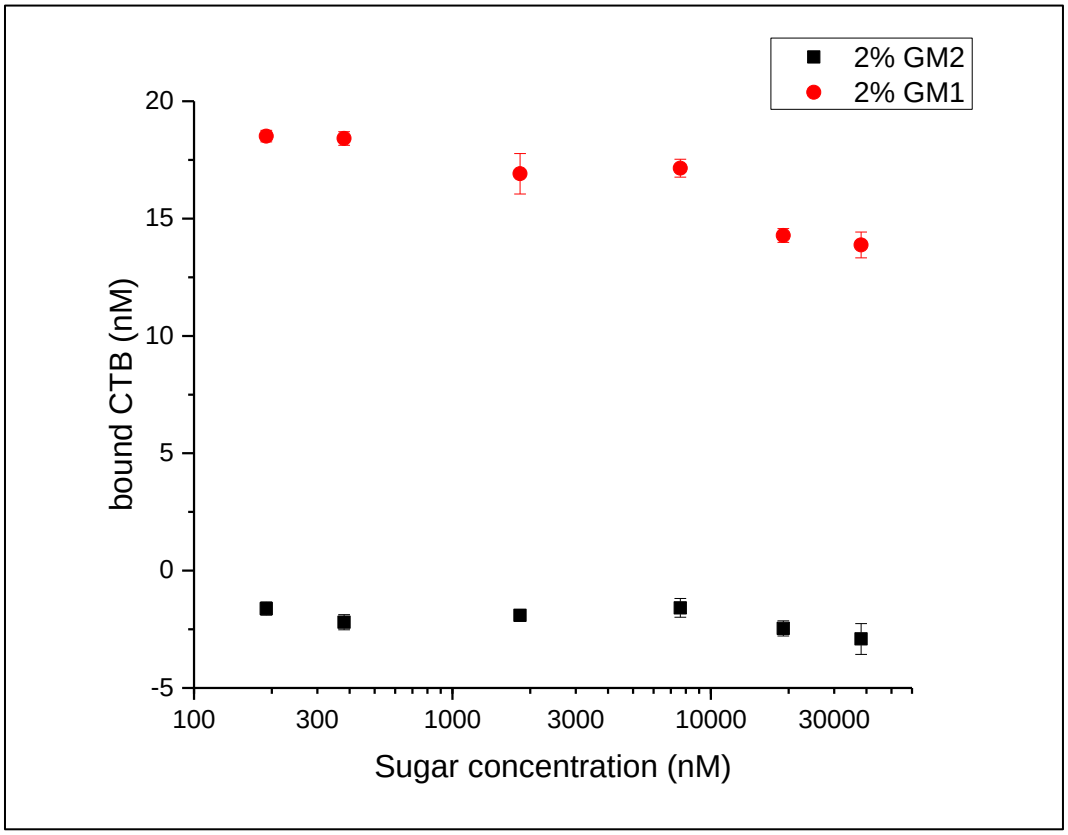

Figure 18. Binding of CTB (prebound with GM_1os) with 2% GM_1 and 2% GM_2

11. FUTURE WORK

11.1 Optimization tool for studying complex interactions

Analyzing complex multivalent binding in heterogeneous mixtures of lipids necessitates the use of an advanced tool to effectively design and study experiments. The binding of biomolecules with heterogeneous mixtures of carbohydrates enables the identification of the optimum mixture composition that maximizes binding. This data may be used to identify possible treatments for diseases where the biomolecule or disease causing agent will bind to a drug covered with a bilayer of this optimum lipid composition rather than the cell membrane of human cells.

For simplicity, two lipids, GM_1 and GM_2 were chosen to make several compositions of a heterogeneous mixture of lipids. The binding capacity at 706 nM of total CTB concentration was studied over three different days. The experiments were repeated thrice to minimize inter-day variability.

A color map has also been made to illustrate the highly nonlinear behavior of binding capacity (Figure 19) and preliminary results obtained have been shown in Table 8. A complex model for understanding this nonlinear behavior will enable the identification of optimum mixture compositions.

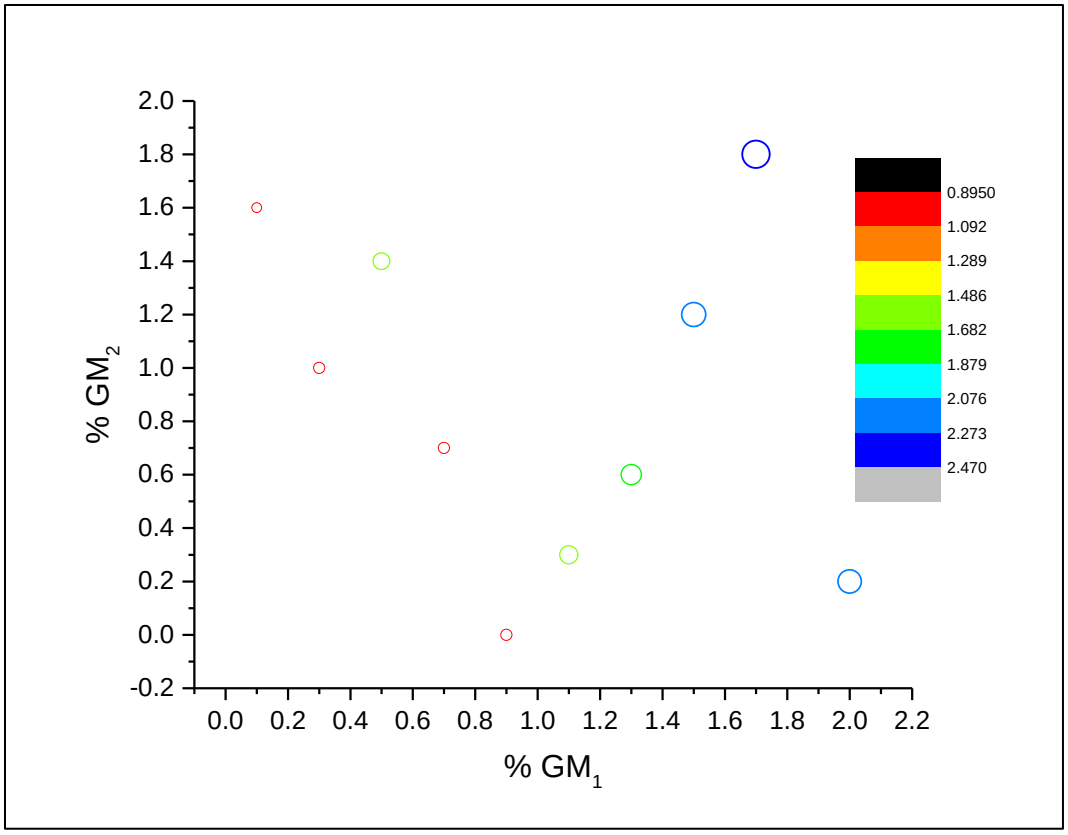

Figure 19. A color map showing the variation in binding capacity for GM_1 and GM_2

Table 8. Preliminary data highlighting the nonlinearity in binding capacity for mixtures of GM_1+GM_2 system

S No.	%GM_1	%GM_2	Day 1	Day 2	Day 3	Average Shift (nm)	Standard Deviation	%Error
1	0.7	0.7	1.02	1.03	0.99	1.02	0.02	1.95
2	1.7	1.8	2.47	2.24	2.70	2.47	0.23	9.24
3	0.1	1.6	0.92	0.79	0.99	0.90	0.10	11.31
4	1.5	1.2	2.22	2.24	2.09	2.18	0.08	3.73
5	0.5	1.4	1.38	1.66	1.47	1.50	0.14	9.50
6	1.1	0.3	1.54	1.83	1.50	1.62	0.18	11.14
7	0.3	1	0.87	1.17	1.02	1.02	0.15	14.88
8	1.3	0.6	1.70	1.82	1.96	1.83	0.13	7.11
9	0.9	0	1.08	0.87	1.09	1.01	0.12	12.30
10	2	0.2	2.11	2.12	2.09	2.11	0.02	0.79

12. CONCLUSION

In conclusion, nanocube sensors were successfully used to quantify the binding of CTB with several gangliosides. Binding capacity of CTB was found to increase on increase the amount of gangliosides. Some gangliosides were found to be positively cooperative and others negatively/ non- cooperative. Cooperativity was found to play a role in determining binding capacity. Mixing different types of ligands gave fascinating results. Weakly binding gangliosides were found to significantly augment binding capacity of CTB in the presence of other strongly binding gangliosides. This demonstrated why protein binding cannot be used to correlate carbohydrate expression. A theoretical model was adapted to explain this interesting phenomenon observed while analyzing multivalent binding with different gangliosides.

The reason such a study was possible was because of the availability of a high throughput tool like the nanocube sensor. This technology allowed multiple replications and testing at several different experimental conditions. This illustrates the importance of such a technology in studying the binding of biomolecules and its potential in discovering treatments for diseases.

REFERENCES

1. WHO. *Cholera*. 2016 4-22-16]; Available from: http://www.who.int/mediacentre/factsheets/fs107/en/.
2. Yu, R.K., et al., *Novel GM1 ganglioside-like peptide mimics prevent the association of cholera toxin to human intestinal epithelial cells in vitro.* Glycobiology, 2016. **26**(1): p. 63-73.
3. WHO. *Ebola virus disease*. 2016 4-22-16]; Available from: http://www.who.int/mediacentre/factsheets/fs103/en/
4. WHO. *Zika virus*. 2016 4-22-16]; Available from: http://www.who.int/mediacentre/factsheets/zika/en/
5. Prevention, C.f.D.C.a. *Zika virus*. 2016 4-22-16]; Available from: http://www.cdc.gov/zika/symptoms/index.html
6. Park, S., et al., *Carbohydrate microarrays.* Chem Soc Rev, 2013. **42**(10): p. 4310-26.
7. Wang, L., et al., *Cross-platform comparison of glycan microarray formats.* Glycobiology, 2014. **24**(6): p. 507-17.
8. Safina, G., *Application of surface plasmon resonance for the detection of carbohydrates, glycoconjugates, and measurement of the carbohydrate-specific interactions: a comparison with conventional analytical techniques. A critical review.* Anal Chim Acta, 2012. **712**: p. 9-29.
9. Ma, Y., et al., *Liposomal glyco-microarray for studying glycolipid-protein interactions.* Anal Bioanal Chem, 2012. **404**(1): p. 51-8.

10. Zhu, X.Y., et al., *Quantitative Glycomics from Fluidic Glycan Microarrays.* Journal of the American Chemical Society, 2009. **131**(38): p. 13646-13650.

11. Worstell, N.C., et al., *Binding Cooperativity Matters: A GM1-Like Ganglioside-Cholera Toxin B Subunit Binding Study Using a Nanocube-Based Lipid Bilayer Array.* PLoS ONE, 2016. **11**(4): p. 1-17.

12. Tao, A., P. Sinsermsuksakul, and P. Yang, *Polyhedral silver nanocrystals with distinct scattering signatures.* Angewandte Chemie - International Edition, 2006. **45**(28): p. 4597-4601.

13. Wu, H.-J., et al., *Membrane-protein binding measured with solution-phase plasmonic nanocube sensors.* Nature Methods, 2012. **9**(12): p. 1189-1191.

14. Near, R., S. Hayden, and M. El-Sayed, *Extinction vs absorption: Which is the indicator of plasmonic field strength for silver nanocubes?* Journal of Physical Chemistry C, 2012. **116**(43): p. 23019-23026.

15. Hong, Y., et al., *Localized surface plasmon resonance based nanobiosensor for biomarker detection of invasive cancer cells*.

16. Zhang, T., et al., *Fabrication and Optical Spectral Characterization of Linked Plasmonic Nanostructures and Nanodevices*.

17. Petryayeva, E. and U.J. Krull, *Localized surface plasmon resonance: Nanostructures, bioassays and biosensing-A review*.

18. Inc., C. *Gold Nanoparticle properties*. 2016 4-23-16]; Available from: http://www.cytodiagnostics.com/store/pc/Gold-Nanoparticle-Properties-d2.htm.

19. Inc., C. *Silver nanoparticles*. 2016 6-1-16]; Available from: http://www.cytodiagnostics.com/store/pc/Silver-Nanoparticle-Properties-d11.htm.

20. Guidelli, E.J., D.R. Clarke, and O. Baffa, *Enhanced UV Emission from Silver/ZnO and Gold/ZnO Core-Shell Nanoparticles: Photoluminescence, Radioluminescence, and Optically Stimulated Luminescence.* Scientific Reports, 2015. **5**.

21. Bharati, K. and N.K. Ganguly, *Cholera toxin: A paradigm of a multifunctional protein.* Indian Journal of Medical Research, 2011. **133**(2): p. 179-187.

22. McDowall, J. *Cholera Toxin*. 2005 4-23-16]; Available from: https://www.ebi.ac.uk/interpro/potm/2005_9/Page2.htm.

23. Ryan, M. and L. Washburn. *Pathogenicity of Cholera*. 2015 [cited 5-31-16; Available from: https://sites.tufts.edu/quorumsensing/qs-in-vibrio-cholerae/pathogenicity-of-cholera/.

24. Todar, K. *Vibrio cholerae and Asiatic Cholera*. 2008 6-1-16]; Available from: http://textbookofbacteriology.net/cholera_3.html.

25. Kuziemko, G.M., M. Stroh, and R.C. Stevens, *Cholera Toxin Binding Affinity and Specificity for Gangliosides Determined by Surface Plasmon Resonance.* Biochemistry, 1996. **35**(20): p. 6375-6384.

26. Lin, H., E. Kitova, and J. Klassen, *Measuring Positive Cooperativity Using the Direct ESI-MS Assay. Cholera Toxin B Subunit Homopentamer Binding to GM1*

Pentasaccharide. Journal of The American Society for Mass Spectrometry, 2014. **25**(1): p. 104-110.

27. Kim, C.S., J.H. Seo, and H.J. Cha, *Functional Interaction Analysis of GM1-Related Carbohydrates and Vibrio cholerae Toxins Using Carbohydrate Microarray.* Analytical Chemistry, 2012. **84**(15): p. 6884-6890.
28. Schengrund, C.L. and N.J. Ringler, *Binding of Vibrio cholera toxin and the heat-labile enterotoxin of Escherichia coli to GM1, derivatives of GM1, and nonlipid oligosaccharide polyvalent ligands.* Journal of Biological Chemistry, 1989. **264**(22): p. 13233-13237.
29. Turnbull, W.B., B.L. Precious, and S.W. Homans, *Dissecting the Cholera Toxin−Ganglioside GM1 Interaction by Isothermal Titration Calorimetry.* Journal of the American Chemical Society, 2004. **126**(4): p. 1047-1054.
30. Shi, J.J., et al., *GM(1) clustering inhibits cholera toxin binding in supported phospholipid membranes.* Journal of the American Chemical Society, 2007. **129**(18): p. 5954-5961.
31. Lauer, S., et al., *Analysis of Cholera Toxin−Ganglioside Interactions by Flow Cytometry†.* Biochemistry, 2002. **41**(6): p. 1742-1751.
32. Schoen, A. and E. Freire, *Thermodynamics of intersubunit interactions in cholera toxin upon binding to the oligosaccharide portion of its cell surface receptor, ganglioside GM1*. Biochemistry, 1989. **28**(12): p. 5019-5024.

33. Jung, H., A.D. Robison, and P.S. Cremer, *Multivalent ligand–receptor binding on supported lipid bilayers.* Journal of Structural Biology, 2009. **168**(1): p. 90-94.

34. MacKenzie, C.R., et al., *Quantitative analysis of bacterial toxin affinity and specificity for glycolipid receptors by surface plasmon resonance.* Journal of Biological Chemistry, 1997. **272**(9): p. 5533-5538.

35. Molander-Melin, M., et al., *Structural membrane alterations in Alzheimer brains found to be associated with regional disease development; increased density of gangliosides GM1 and GM2 and loss of cholesterol in detergent-resistant membrane domains.* Journal of Neurochemistry, 2005. **92**(1): p. 171-182.

36. Leney, A.C., et al., *Nanodiscs and Electrospray Ionization Mass Spectrometry: A Tool for Screening Glycolipids Against Proteins.* Analytical Chemistry, 2014. **86**(11): p. 5271-5277.

37. Castellana, E.T. and P.S. Cremer, *Imaging large arrays of supported lipid bilayers with a macroscope.* Biointerphases, 2007. **2**(2): p. 57-63.

38. Tanaka, M. and E. Sackmann, *Polymer-supported membranes as models of the cell surface.* Nature, 2005. **437**(7059): p. 656-663.

39. Giuliani, A., et al., *The different inhibiting effect of cholera toxin on two leukemia cell lines does not correlate with their toxin binding capacity.* Molecular and Cellular Biochemistry, 1995. **152**(2): p. 103-112.

40. Dawson, G., *Measuring brain lipids.* Biochimica et Biophysica Acta (BBA) - Molecular and Cell Biology of Lipids, 2015. **1851**(8): p. 1026-1039.

41. Yanagisawa, M. and R.K. Yu, *The expression and functions of glycoconjugates in neural stem cells.* Glycobiology, 2007. **17**(7): p. 57R-74R.

42. Yanagisawa, M., T. Ariga, and R.K. Yu, *Letter to the Glyco-Forum: Cholera toxin B subunit binding does not correlate with GM1 expression: a study using mouse embryonic neural precursor cells.* Glycobiology, 2006. **16**(9): p. 19G-22G.

43. Lin, H., E.N. Kitova, and J.S. Klassen, *Measuring positive cooperativity using the direct ESI-MS assay. Cholera toxin B subunit homopentamer binding to GM1 pentasaccharide.* J Am Soc Mass Spectrom, 2014. **25**(1): p. 104-10.

44. Perez, S. *The Symbolic Representation of Monosaccharides in the Age of Glycobiology*. 2014 5-31-16]; Available from: http://glycopedia.eu/e-chapters/the-symbolic-representation-of/article/at-the-instigation-of-glycobiology.

45. Hlavacek, W.S., R.G. Posner, and A.S. Perelson, *Steric Effects on Multivalent Ligand-Receptor Binding: Exclusion of Ligand Sites by Bound Cell Surface Receptors.* Biophysical Journal. **76**(6): p. 3031-3043.

46. Jin, X., J. Talbot, and N.H.L. Wang, *Analysis of steric hindrance effects on adsorption kinetics and equilibria.* AIChE Journal, 1994. **40**(10): p. 1685-1696.

47. Jung, H., A.D. Robison, and P.S. Cremer, *Multivalent ligand-receptor binding on supported lipid bilayers.* J Struct Biol, 2009. **168**(1): p. 90-4.

48. Hardt, S.L., *Rates of diffusion controlled reactions in one, two and three dimensions.* Biophysical Chemistry, 1979. **10**(3-4): p. 239-243.

49. Williamson, M.P., *How proteins work. Mike Williamson*. 2012: New York : Garland Science, [2012].

50. Rich, A., N.R. Davidson, and L. Pauling, *Structural chemistry and molecular biology. Edited by Alexander Rich and Norman Davidson*. 1968: San Francisco : W. H. Freeman, [1968].